Archean Protolith and Accretion of Crust in Kamchatka: SHRIMP Dating of Zircons from Sredinny and Ganal Massifs

I. N. Bindeman, V. I. Vinogradov,[1] J. W. Valley, J. L. Wooden,[2] and B. A. Natal'in[3]

Department of Geology and Geophysics, University of Wisconsin—Madison, Madison, Wisconsin 53706, U.S.A.
(e-mail: inbindem@geology.wisc.edu)

ABSTRACT

We used an ion microprobe (SHRIMP-RG) for U-Pb dating of individual zircons in high-grade metamorphic basements of the felsic Sredinny and mafic Ganal Massifs in Kamchatka. Thirty percent of zircons from paragneisses of the Sredinny Massif contain Archean (2800–2500 Ma), early Proterozoic (1700–2100 Ma), and late Proterozoic (~1000 Ma) detrital cores. In addition, a broad and almost uninterrupted range of Phanerozoic detrital cores (460–175 Ma) is present, with Jurassic to Lower Cretaceous (150–96 Ma) zircons forming the youngest detrital age group. Ubiquitous 77 ± 2-Ma rims signify the age of regional metamorphism, though yet another metamorphism is defined by four 47–53-Ma zircons. The abundance of Archean, Proterozoic, and Paleozoic zircon cores, as well as the short ~20-m.yr. time lag between the youngest detrital zircon cores and the age of metamorphic rims, argues strongly against a long trans-Pacific transport and the origin of the Sredinny Massif as a piece of a continent other than Siberia. We suggest that the Sredinny Massif is an eastern part of the exposed basement (leading edge) of the Sea of Okhotsk (Okhotomorsk) microcontinent and that it represents a polymetamorphic accretionary wedge whose clastic sediments were derived from Siberia. Zircon ages from amphibolites and gabbro in the Ganal Massif exhibit two age groups, one at 60–80 Ma and the other at 18–40 Ma, and lack Precambrian cores. We interpret the Ganal Massif as the lower crust of an intraoceanic island arc. The Sredinny and Ganal Massifs, despite their present proximity, belong to different tectonic units and do not represent upper and lower crustal fragments of the same unit. We present a tectonic model that explains the origin of both Massifs as a part of Mesozoic and Cenozoic geodynamic history in the NW Pacific.

Introduction

This study aims to constrain the time of accretion of crust in the Kamchatka Peninsula, Russia, and to find a source continent for metasedimentary rocks exposed in the Sredinny and Ganal Massifs (fig. 1). Crustal accretion in Kamchatka is critical for understanding the Late Mesozoic–Cenozoic plate tectonic evolution of the NW Pacific and for formation of the present-day Kurile-Kamchatka-Aleutians subduction pattern. We use ion microprobe analysis of Pb, U, and Th isotopes in cores and rims of zircons extracted from the metasedimentary rocks because we believe that this method is best for determining the protolith age, the likely source continent, and the age of metamorphism(s)

in these massifs. We use these data to interpret the tectonic history of Kamchatka accretion.

Regional Tectonic Context

Identification, origin, transportation, and emplacement of terranes in the north Circum–Pacific have been a subject of long controversy (e.g., Watson and Fujita 1985; Parfenov and Natal'in 1986; Rowley 1992; Nokleberg et al. 1998; Bogdanov and Khain 2000). Geodynamic theories on the mechanisms of transport and accretion of the north Circum–Pacific vary widely and can be classified into intraoceanic, with the ocean plate transport models (Konstanti-novskaia 2000, 2001; Levashova et al. 2000), and coast-wise translation transport models (e.g., Na-tal'in et al. 1986; Geist et al. 1994). The abundance of ocean plateaus and islands in the Pacific suggests that episodes of collision and accretion of these terranes to continental margins might have been fre-
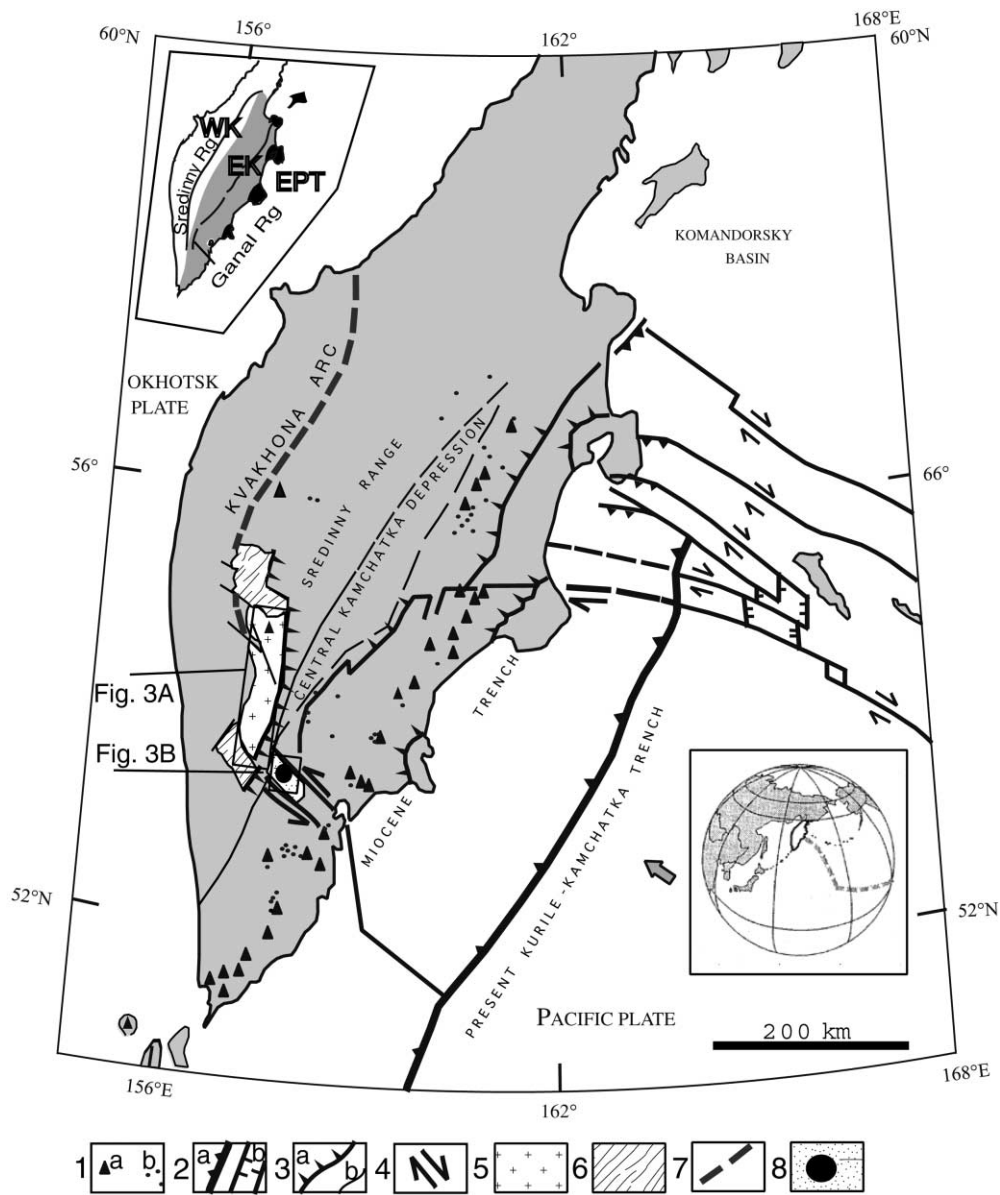
Figure 1. Tectonic setting of the Sredinny and Ganal Massifs in Kamchatka. Kamchatka/Aleutian junction is modified after Gaedicke et al. (2000). Onland geology is after Bogdanov and Khain (2000). 1, Active volcanoes (*a*) and Holocene monogenic vents (*b*). 2, Trench (*a*) and pull-apart basin in the Aleutian transform zone (*b*). 3, Thrust (*a*) and normal (*b*) faults. 4, Strike-slip faults. 5–6, Sredinny Massif. 5, Amphibolite-grade felsic paragneisses of the Kolpakovskaya series. 6, Allochthonous metasedimentary and metavolcanic rocks of the Malkinskaya series. 7, The Kvakhona arc. 8, Amphibolites and gabbro (*solid circle*) of the Ganal Massif. Lower inset shows the global position of Kamchatka. Upper inset shows main Cretaceous-Eocene tectonic units (Bogdanov and Khain 2000): Western Kamchatka (*WK*) composite unit including the Sredinny Massif, the Kvakhona arc, and the thick pile of Upper Cretaceous marine clastic rocks; Eastern Kamchatka (*EK*) arc, and Eastern Peninsulas terranes (*EPT*). Eastern Kamchatka is also known as the Olyutorka-Kamchatka arc (Nokleberg et al. 1998) or the Achaivayam-Valaginskaya arc (Konstantinovskaya 2000), while Eastern Peninsulas terranes are also called Kronotskaya arc (Levashova et al. 2000).

quent in the past. Seamounts with Paleozoic corrals were found within the Mesozoic foldbelts on the Pacific side of northern Asia (e.g., Sengör and Natal'in 1996). Establishing the past trajectories and kinematics of transport of accreted terranes requires an integral geologic and geochronologic approach.

In western North America, strongly oblique subduction since the end of the Early Cretaceous (Engebretson et al. 1985) is responsible for rapid (>5 cm/yr) coast-parallel translation of island arc terranes (e.g., Beck 1986, 1991), which can be facilitated by arc plutonism causing strain partitioning (Sant Blanquat et al. 1998). In the NW Pacific, the convergence character was different. Subduction under Eurasia has been in a NW direction for at least the past 80 m.yr. based on the plate kinematics (Engebretson et al. 1985) and the Hawaii–Emperor Chain hotspot track. Periods of small angle oblique convergence of the Pacific, Farallon, and Kula plates with Eurasia alternated with periods of nearly orthogonal subduction. The subduction was mostly head-on at ca. 90° after ca. 43 Ma but was more oblique (left lateral) in the Late Cretaceous–Eocene time (80–43 Ma; Engebretson et al. 1985). However, if Late Cretaceous–Paleogene intraoceanic arcs did exist in the Pacific (e.g., Konstantinovskaya 2000, 2001; Levashova et al. 2000), the kinematic history of subduction zones at the eastern margin of Eurasia cannot be deduced from magnetic anomalies and hotspot traces preserved in the Pacific ocean. Left lateral, Cretaceous strike-slip motion is regional in the NW Pacific and was recognized in far-eastern Russia (Natal'in et al. 1986; Natal'in 1993) and Japan (e.g., the Median Tectonic Line of Japan; Faure et al. 1986; Taira et al. 1989).

Kamchatka Peninsula

The Kamchatka Peninsula, Russia, is separated from the Siberian craton by 1200 km and is isolated from it by the mid to Late Cretaceous Okhotsk-Chukotsk belt and Triassic–Early Cretaceous Uda-Murgal magmatic arc and related accretionary wedges (fig. 2). Kamchatka consists of the Western Kamchatka, Eastern Kamchatka, and Eastern Peninsulas terranes (Bogdanov and Khain 2000; fig. 1).

The Cenozoic assembly of Kamchatka is interpreted to be the result of progressive terrane accretion from the southeast (Zonenshain et al. 1990; Geist et al. 1994; Garver et al. 2000; Levashova et al. 2000). Eastern Kamchatka and Eastern Peninsulas terranes originated in the Late Cretaceous as intraoceanic island arcs >2000 km outboard at 38°–45°N based on paleontologic and paleomagnetic data; Eastern Kamchatka accreted to Western Kamchatka

in the Early Eocene, while the Eastern Peninsulas terranes arrived in the end of Miocene (see Konstantinovskaya 2000, 2001; Levashova et al. 2000). However, the plate to which they belonged (Kula, Pacific, North American, or Eurasian), subduction polarity, and the trajectory of the movements are debated (e.g., Levashova et al. 2000).

The oldest rocks of Western Kamchatka are believed to be high-grade metamorphic rocks of the Sredinny Massif. The Sredinny Massif is considered to be part of the larger Okhotomorsk block underlying the central part of the Sea of Okhotsk (Parfenov et al. 1978; Parfenov and Natal'in 1986; Konstantinovskaya 2000, 2001). In the west, the Sredinny Massif is tectonically overlain by the Late Jurassic to Early Cretaceous Kvakhona arc (Bondarenko and Sokolov 1990; Remizovsky et al. 1993; Konstantinovskaya 2000). Views on the origin of Western Kamchatka vary widely and include a Mesozoic intraoceanic transport and accretion to Asia (Parfenov et al. 1978; Parfenov and Natal'in 1986; Zonenshain et al. 1990) as well as a largely in situ origin (Sidorenko 1964; Markov 1975; Khanchuk 1985). Any tectonic interpretations of the origin and the past trajectories of Western Kamchatka should consider the nature, timing, and the mechanism of accretion of the Okhotomorsk block (see fig. 2). Unlike the Sea of Japan, which has clearly oceanic crust (e.g., Jolivet et al. 1994), crust under the Sea of Okhotsk is characterized by variable but largely "continental" thickness (20–30 km) and seismic velocities (Gnibidenko and Khvedchuk 1982; Bogdanov and Khain 2000). The crust, however, is stretched, faulted, and covered with thick (1 to >6 km) Cenozoic sediments (Bogdanov and Khain 2000). No drilling has penetrated deep enough to sample the metamorphic basement in the Sea of Okhotsk. Greenschists, phyllites, sandstones, cherts, intermediate and acid volcanic rocks, and various granitoids have been dragged from the uplift in the central part of the Sea of Okhotsk (Gnibidenko and Khvedchuk 1982; Sergeev and Krasny 1987). These rocks may represent subduction-accretion complexes invaded by migrating magmatic fronts (Sengör and Natal'in 1996). The Late Cretaceous/early Eocene collision of the Okhotomorsk block caused cessation of subduction along the extensive Okhotsk-Chukotsk volcanic belt on the continental margin of Asia (fig. 2) and forced subduction to jump outboard many hundreds kilometers to the east (e.g., Parfenov and Natal'in 1986; Geist et al. 1994; Kimura 1994; Nokleberg et al. 1998).
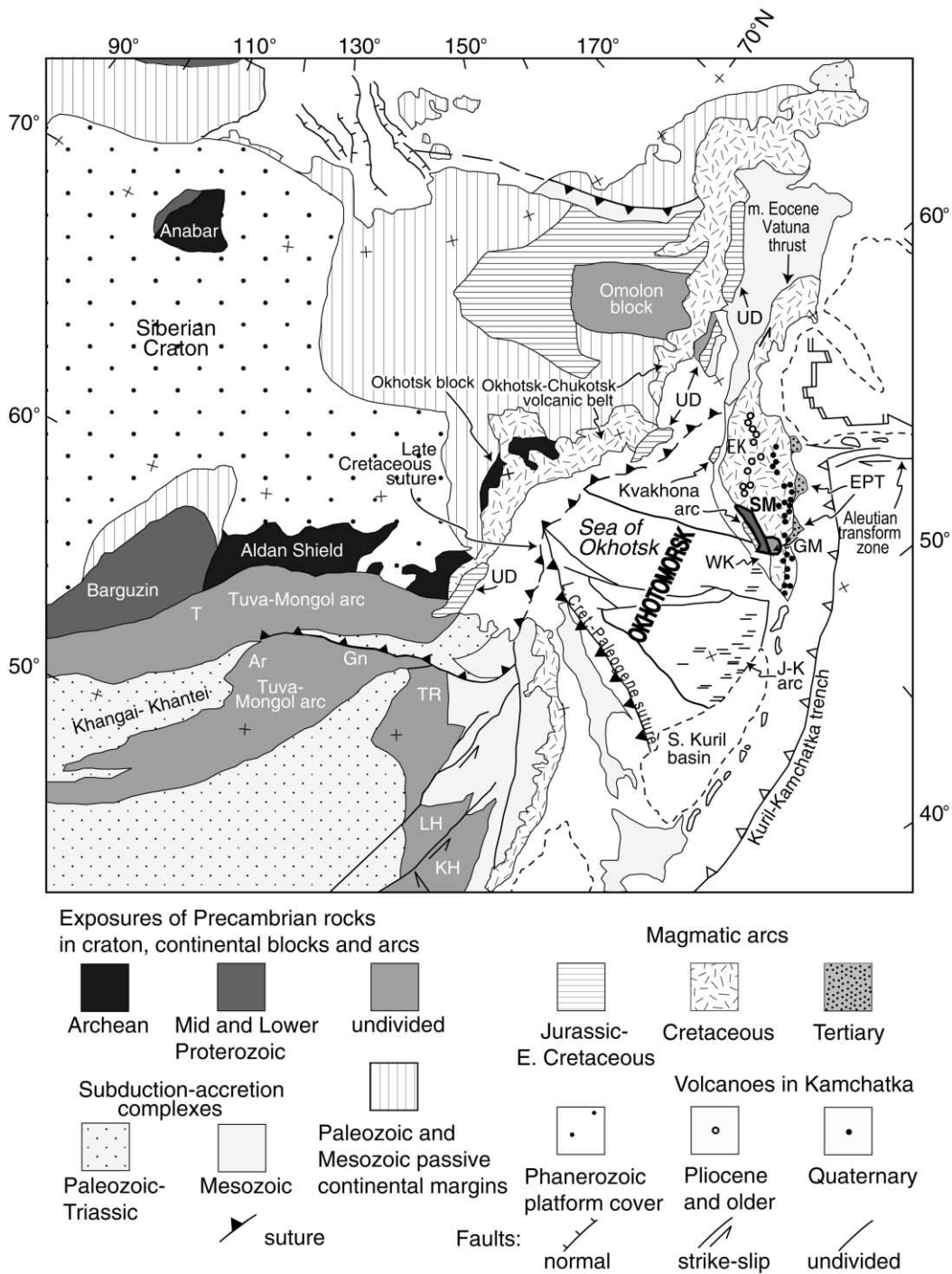
Figure 2. Position of the Sredinny (*SM*) and Ganal (*GM*) Massifs in the tectonic framework of the northeastern Russia and possible source areas for Archean and Proterozoic detrital zircons. Tectonic units are modified after Sengör and Natal'in (1996). Spreading center in the Komandorsk basin is after Baranov et al. (1991). The Aleutian transfer fault zone is after Gaedike et al. (2000). Note that the platform cover of the Siberian craton starts with the late Proterozoic; therefore only the Aldan shield and Anabar arch could be source areas for early Precambrian detrital zircons in Phanerozoic deposits. The Paleozoic to early Mesozoic Tuva-Mongol arc forms the orocline enveloping the Paleozoic to Early Mesozoic subduction-accretionary complexes. The hinge of the orocline is located to the west of the figure area. In the Tuva-Mongol arc as well as in continental blocks to the southeast of the arc (*TR*, Turan; *LH*, Lesser Hingan; and *KH*, Khanka), Archean and Proterozoic rocks are exposed among large Paleozoic and Mesozoic

Crust and Crystalline Complexes of Kamchatka

The age and origin of the crust under Kamchatka has long been controversial. Seismic data indicate the presence of 30–45-km-thick continental crust, crust thicker than that in the Sea of Okhotsk and neighboring oceanic island arcs (Bogdanov and Khain 2000). Geologists believe that gneisses and amphibolites form much of the basement under the Kamchatka Peninsula; occurrence of xenoliths in recent volcanic rocks supports this view (Volynets et al. 1987).

Outcrops of metamorphic complexes are exposed in the Sredinny and Ganal Massifs (figs. 1, 3), which are likely to represent the basements of Western and Eastern Kamchatka, respectively. The Sredinny Massif (SM; 200 × 40 km) crops out in the center of the Sredinny range of Western Kamchatka and predominantly comprises migmatized felsic gneisses. The Ganal Massif (GM; 60 × 20 km) in Eastern Kamchatka consists of mafic amphibolites and a gabbroic intrusion. Sredinny Massif and GM are separated by the 600-km-long, Central Kamchatka depression (fig. 1). Both massifs are bound by normal and thrust faults (fig. 1; Rikhter 1991, 1995; Bogdanov and Khain 2000), and in both massifs, metamorphic high-grade basement rocks are variously overlain by Upper Cretaceous–Paleocene (SM) and Eocene (GM) greenschist facies metavolcanic and metasedimentary rocks and by Cenozoic volcanic rocks. The metamorphic rocks of this cover are poorly dated; fossils have been recovered from Late Paleocene and Oligocene sedimentary and volcanic units on SM and from Eocene sedimentary units on GM. (Details are in the appendix, which is available free of charge from the *Journal of Geology* office.)

The basement of SM comprises migmatized quartz and plagioclase (Qz-Pl) and kyanite-bearing gneisses and schists belonging to the Kolpakovskaya series (>2500-m thick; Khanchuk 1985; fig. 3A). Mineral parageneses of the series reveal a complex polymetamorphic history (e.g., Khanchuk 1985). Rb-Sr whole-rock dating of rocks from the Kolpakovskaya series yielded two groups of ages: 110–140 Ma and 60–70 Ma as well as uniformly low $^{87}Sr/^{86}Sr_i$ of 0.703–0.706 (Vinogradov et al. 1988;

Vinogradov and Grigoryev 1994). The oldest Rb-Sr whole-rock age of the amphibolite to greenschist facies rocks of the allochthonous Malkinskaya series (which overthrust the Kolpakovskaya series; see appendix) clusters around 70 Ma, signifying a 50-Ma time gap between the oldest metamorphic events in the Kolpakovskaya and Malkinskaya series. At 47 Ma, both series were affected by retrograde metamorphism; this is evidenced from Rb-Sr dating of biotite in plagioclase gneiss of Malkinskaya (Bondarenko et al. 1993) and Kolpakovskaya series (Vinogradov et al. 1988; Vinogradov and Grigoryev 1994).

The basement of GM comprises the Ganal series rocks forming a dome-shaped structure with a Yurchik gabbro-norite pluton in its center (fig. 3B). The Ganal series is mostly composed of metabasalts (amphibolites, garnet amphibolites, epidote-plagioclase schists) with rare horizons of quartzite and marbles. Its structural thickness exceeds 4000 m (German 1978). The $^{40}Ar/^{39}Ar$ dating of amphibolites yielded ages from 52 to 47 Ma, while the Yurchik gabbro yielded ages from 52 to 35 Ma (Zinkevich et al. 1993). Whole-rock Sm-Nd and Rb-Sr isochron ages of gabbro, amphibolites, and orthogneisses (fig. 3B), as well as internal (mineral) isochron dating of the Yurchik gabbro and granulites, yielded zero age (±20 m.yr.), which is more consistent with the post-early Miocene metamorphic event (Vinogradov et al. 1991).

A variety of whole-rock and bulk mineral techniques have been employed to date Kamchatkan metamorphic rocks; these techniques have yielded ages ranging from the Miocene to Proterozoic (see Bogdanov and Khain 2000). The quality of published data is variable; critical assessment of K-Ar geochronology before 1985 is given by Watson and Fujita (1985). Neither single crystal $^{40}Ar/^{39}Ar$ nor single zircon analyses have been performed on any metamorphic rocks in Kamchatka, even though such analyses would be most appropriate given the complex polymetamorphic history of the Kamchatka rocks. In this study, we choose in situ dating of zircons by ion microprobe as the best method for determining the protolith age (zircon cores) and the age of metamorphism (zircon rims). In the SM and GM, we studied only the structurally lowest

---

granitic plutons indicating extensive and deep erosion. These areas could be good candidates for source areas of Precambrian and Paleozoic detrital zircons. Late Cretaceous and Paleogene sutures separate these source areas from the Okhotomorsk continental block and *SM* and *GM*. Other abbreviations are as follows: *EK*, Eastern Kamchatka arc; *EPT*, Eastern Peninsula arc; *WK*, West Kamchatka composite tectonic unit; *T, Ar*, and *Gn*, Transbaikal, Argun, and Gonzha segments, respectively, of the Tuva-Mongol arc; *UD*, Uda-Murgal arc.
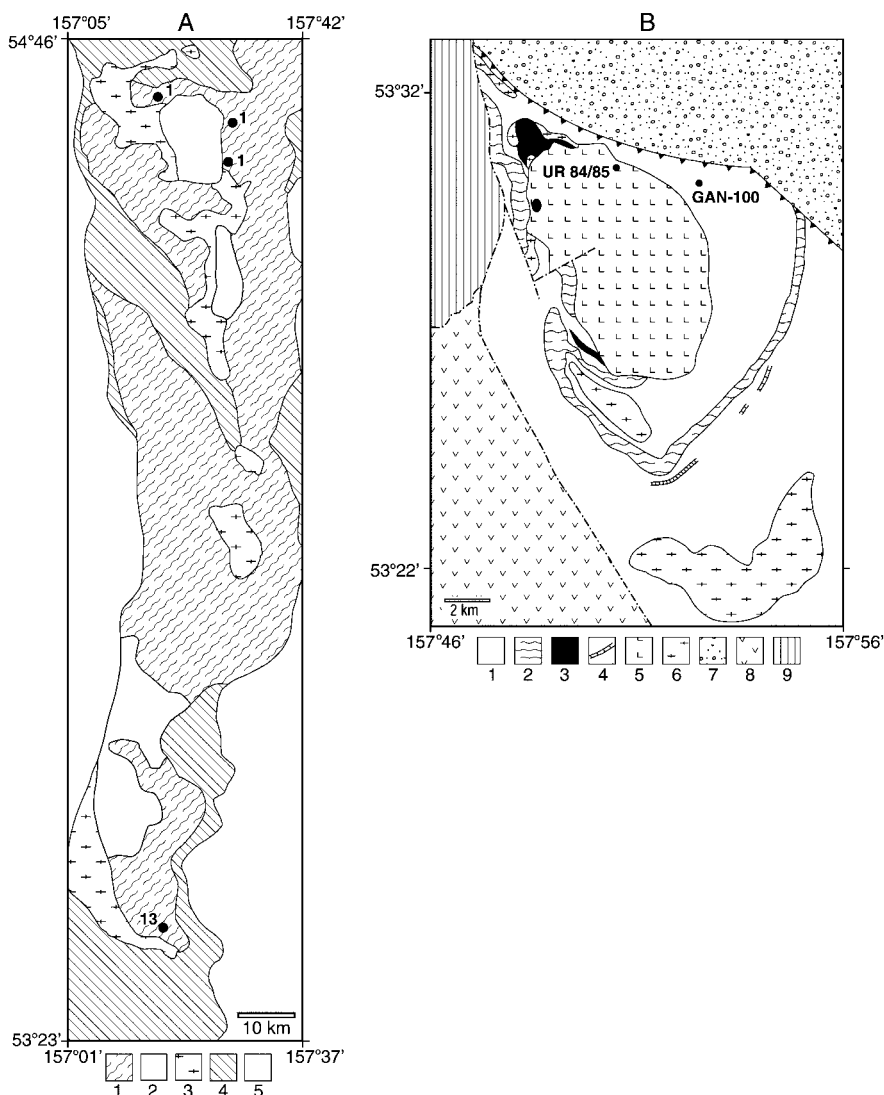
Figure 3. Simplified maps of Sredinny and Ganal Massifs with sample localities. *A*, Sredinny Massif (after VSEGEI 1981); see table 1 for analyses. Combined sample KHAN-1 was collected in an area around Khangar caldera at localities marked 1, which have yielded whole-rock Rb-Sr isochrons of 127–116 Ma (Vinogradov and Grigoryev 1994). Sample KHAN-13 is from a single outcrop 13, which yielded a whole-rock Rb-Sr isochron of 69 ± 8 Ma. 1, Kolpakovskaya series (migmatized paragneisses). 2, Orthogneisses g_1MZ. 3, Orthogneisses g_2MZ. 4, Overlying allochthonous Malkinskaya formation (Kheyvanskaya suite). 5, Miocene-Quaternary volcanic rocks. *B*, Ganal Massif (after German 1978; Richter 1995). 1–4, Ganal series. 1, Amphibolites. 2, Marker horizon of leucocratic metaterrigenous rocks. 3, Mafic granulites. 4, Marker horizons of siliceous marbles. 5, Yurchik gabbro-norite pluton. 6, Orthogneisses. 7, Polymetamorphic rocks of Stenovaya series (greenschist to amphibolite grade). 8, Irunei suite greenschist rocks. 9, Cenozoic volcanic rocks.

and geochronologically oldest series (Kolpakov-skaya and Ganal, respectively); this gave us the best assessment of the protolith ages, their provenance, and, consequently, the origin of the metamorphic basement of the Western Kamchatka and Eastern Kamchatka. The ion microprobe zircon ages provide the first detailed insight into Kamchatka geo-chronology and are essential for critical assessments of proposed tectonic models.

Methods

Sample Selection. In this study, we pursue the goal of getting a broad look into the geochronology

of large, geologically complicated, and insufficiently studied Kamchatkan metamorphic terranes. We concentrated on provenance of detrital zircons that represent regional sampling of a single suite of metasedimentary rocks collected in several outcrops rather than on performing a detailed study of a single sample. The rock samples selected for zircon extraction were originally dated with whole-rock Rb-Sr and Sm-Nd techniques (Vinogradov et al. 1988, 1991; Vinogradov and Grigoryev 1994), which allows comparison of zircon metamorphic ages with whole-rock ages of metamorphism.

Zircons were separated from four samples, two each from SM and GM (fig. 3). One sample of migmatized paragneisses is a composite of 15 rocks from three localities in the Kolpakovskaya series in the north of SM (fig. 3*A*, KHAN-1). This sample was collected in several outcrops with varying degrees of migmatization, proportions of mafic and felsic minerals (and thus Rb/Sr ratio) which previously defined an isochron of 127 ± 6 Ma (Vinogradov and Grigoryev 1994). The second sample was collected from a single outcrop of the Kolpakovskaya series in the southern part of the SM (150 km to the south, sample KHAN-13). It is a composite of 39 hand specimens that defined a whole-rock Rb-Sr isochron of ~65 Ma (Vinogradov and Grigoryev 1994).

In the GM, zircons were extracted from 20 individual hand specimens of amphibolites that had been collected from a single outcrop varying in mafic/felsic mineral proportions of the Ganal series (sample GAN-100). The second sample of zircons came from a single hand specimen of the gabbroic Yurchik pluton (sample UR-84/85). The Yurchik gabbro and the Ganal series rocks yielded zero whole-rock Sm/Nd and Rb/Sr ages (Vinogradov et al. 1991).

Analytical Technique. Zircons were extracted from crushed rocks by conventional techniques involving density and magnetic separation and were then mounted in epoxy and polished and coated with ~10 nm of gold. Before gold coating the zircons, we photographed them in transmitted light to identify undesirable near-surface melt or mineral inclusions and then imaged them by cathodoluminescence to identify cores and rims. The SHRIMP-RG (sensitive, high-resolution, ion microprobe, reverse geometry) at Stanford University provides higher mass resolution and transmission and better accuracy than other ion microprobes. The ~8-nA primary beam of $^{16}O_2^-$ ions produced ~30 μm in diameter, ~1 μm deep, flat-bottomed analysis pits. Before each analyses, we rastered the beam for 3 min to remove the surface contamination. In each spot, data were collected

during 3–6 scans for peaks of $^{90}Zr_2O$, ^{204}Pb, ^{206}Pb, ^{207}Pb, ^{208}Pb, ^{238}U, $^{232}Th^{16}O$, and $^{238}U^{16}O$. Zircon standard AS-57 (1099 Ma; Paces and Miller 1993) was analyzed every four analyses. Zircon standard SL13 was used as a check for U concentrations. We report ^{204}Pb- and ^{207}Pb (common lead)-corrected ages (see table 1, which is available free of charge from the *Journal of Geology*'s Data Depository), and in most cases, the ages are coincident within error. We use the $^{206}Pb/^{238}U$ age for samples younger than 1 Ga and $^{207}Pb/^{206}Pb$ age for those >1 Ga ("preferred age" in table 1). During the first part of the analytical session, we purposely selected grains based on differing size, CL pattern, and zoning; later we analyzed randomly selected grains. Age distribution is remarkably similar in preselected and randomly selected grains, which suggests little or no introduced bias on age distribution pattern. In each sample, we analyzed zircon cores to obtain information on the protolith age, while analyses of zircon rims in metasedimentary rocks provided the age of metamorphic zircon growth. We used ISOPLOT (Ludwig 2000) for plotting concordia diagrams and for identification of age peaks using cumulative probabilities.

Following analysis, we examined zircons of each age group with respect to their external shape, size, cathodoluminescence intensity both in core and rim, zoning pattern, Th and U concentrations, Th/U ratios, presence or absence of the oscillatory zoning, and degree of resorption. Results are summarized in table 1. Little or no correlation can be found between any of these parameters and age. Nonetheless, distinctive inherited, often rounded, and likely detrital cores can be identified in >50% of zircons in SM paragneisses; and these cores can be used in interpretation of protolith age. Such cores are absent in the amphibolites of the GM.

Results

Sredinny Massif. A total of 62 analyses on 57 zircons was performed in two composite samples from the Kolpakovskaya series of the SM (table 1; fig. 4). Regardless of the area, the majority of zircons reveal the same crystallographic shape: doubly-terminated octahedral prisms with acute angle pyramids but with no correlation of shape to the age of the cores. The remaining zircons are either smaller euhedral crystals or irregular grains without visible prismatic overgrowth (table 1).

Cathodoluminescence (CL) intensity, zoning pattern, and resorption features inside zircons were used to identify cores. Zircon cores, often eccentrically positioned, can be recognized in most zircons, but the shape, degree of rounding, CL pattern,

Sredinny Massif:

Sample KHAN-13

Sample KHAN-1

Ganal Massif:

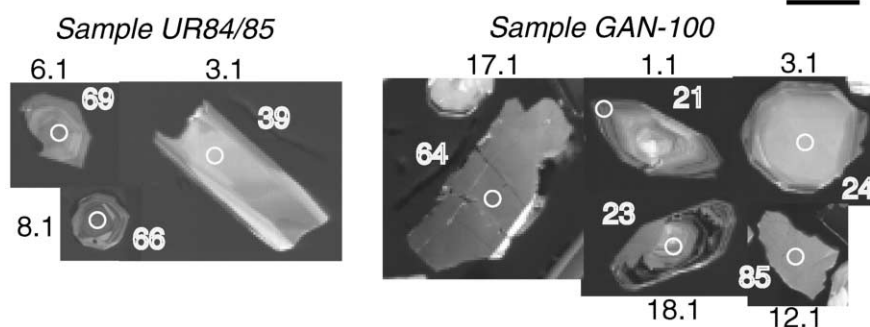### Sample UR84/85

Sample GAN-100
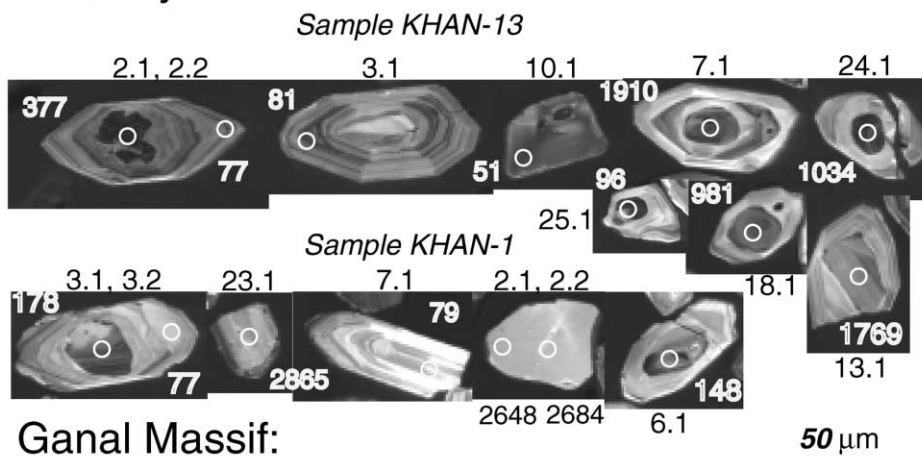
Figure 4. Cathodoluminescence images of analyzed zircons from the Sredinny and Ganal Massifs. See figure 3 for sample localities, table 1 for analyses, and text for discussion. Decimal numbers (e.g., 3.1) refer to spot number in table 1; rounded numbers (e.g., 1910) are U-Pb ages in millions of years.

Th and U concentrations, and Th/U ratio vary widely (table 1; fig. 4). Little can be inferred on the origin and degree of transport abrasion of inherited cores since many cores in SM bear evidence of high-temperature resorption and blurring of original CL patterns (e.g., Nemchin and Pidgeon 1997; Schaltegger et al. 1999). Nonetheless, many zircons contain cores with oscillatory zoning (which is most common in igneous zircons), and others are clearly metamorphic—they have extremely low (<0.1) Th/U ratio and/or dull CL without oscillatory zoning. Analyses with low Th/U of any age result from relatively high U content (300–1400 ppm) and moderately low Th content (30–200 ppm).

The majority of analyzed zircons are concordant within error on conventional (Wetherill) and inverse (Tera-Wasserburg) concordia diagrams (fig. 5). Several discordant analyses represent analyses of inner rims with core/rim overlap of analyzed spot (table 1). Zircon cores in paragneisses in the Kolpakovskaya series from the south and the north of the SM show similar age distribution (fig. 6A, 6B).

Therefore, a cumulative age distribution for SM is discussed below (fig. 6C, 6D).

Zircon cores can be grouped by age. More than 30% of detrital zircon cores are Precambrian with distinct Archean (2800–2500 Ma), Lower Proterozoic (1700–2100 Ma), and Upper Proterozoic (~1000 Ma) age peaks (fig. 6D). The rest are represented by a broad and almost uninterrupted range of Phanerozoic ages (460–175 Ma). Abundant Jurassic to Lower Cretaceous (150–120 Ma) cores form the youngest detrital age group; this is a significant finding that we will discuss later.

The oldest Archean group of zircons in the SM (four cores, five analyses, 8% of total population of 62 analyses) is represented by inconspicuous, irregularly shaped, or broken grains with medium CL and obliterated zoning (table 1). The Lower Proterozoic group comprises 12 cores (19%) with both regular and highly irregular resorbed core morphology with predominantly dark to medium-dark CL and no internal zoning. Two Upper Proterozoic grains of 1000 Ma have extremely low (metamor-
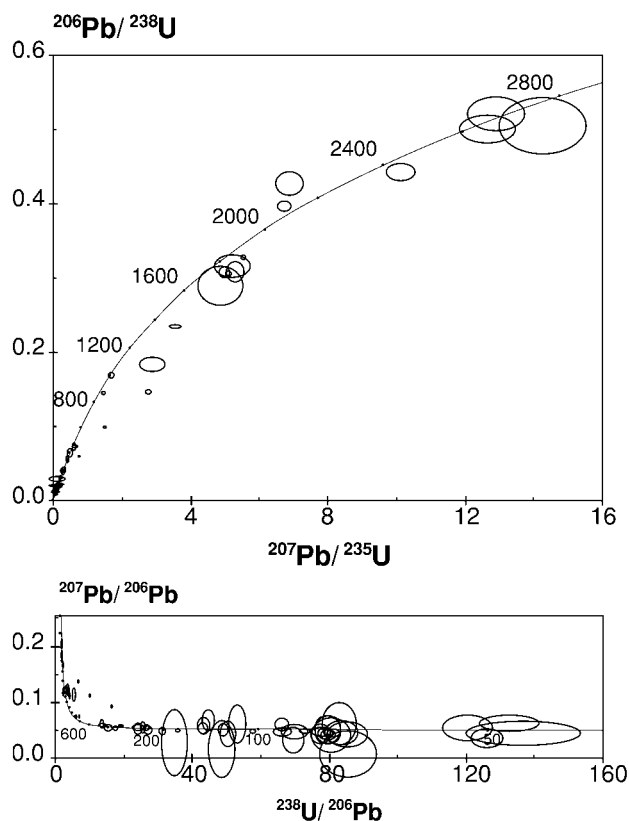
Figure 5. Conventional (Wetherill, above) and inverse (Tera-Wasserburg; below) concordia diagrams for zircon analyses in Qz-Pl gneisses of the Sredinny Massif samples Khan-1 and Khan-13. Note that most analyses are concordant and span a wide range of ages; $\pm 2\sigma$ error ellipses are shown.

phic) Th/U ratio (0.1 and 0.05), dull CL, and no zoning.

Zircon cores with a wide range of Paleozoic to Jurassic ages 460–175 Ma (15 zircons, 24%) are characterized by the predominance of oscillatory (igneous) zoning with CL of variable intensity. The Jurassic–Lower Cretaceous (120–150 Ma) detrital age peak includes the group of eight cores (13%). These cores have dark CL and oscillatory zoning and are distinctly sharply bounded against overgrowth with age of 77 Ma. The youngest detrital cores are two 96-Ma zircons (fig. 4).

Seventeen analyses (27%) of zircon ages cluster in the 96–75-Ma range, with the maximum number of ages at 77 ± 2 Ma (fig. 6D); 77 Ma is the age of rims of seven euhedral crystals and also the dominant and narrowly defined age of the centers of six zircon crystals with no inherited cores. Two older zircon analyses of this group (92–88 Ma) show older rounded cores that are surrounded by a 77-Ma rim,

but these older ages result from the partial overlap of ion microprobe pits onto older cores. Zircons of the 77-Ma group exhibit the most regular pattern of internal oscillatory zoning of medium to light CL intensity and are characterized by an octahedral prismatic shape. The morphology and CL pattern of the 13 zircons at 75–82 Ma is similar to the CL pattern of rims of most other analyzed zircon crystals with older cores; this supports the observation that the majority of older zircon cores are overgrown by ca. 77-Ma rims.

The euhedral shape of most 77-Ma zircons is consistent with unconstrained growth in leucosomes during peak-metamorphic anatexis (e.g., Vavra et al. 1996). The anhedral shape of a few 77-Ma zircons could represent either resorption after the peak metamorphism or zircon shielding by other minerals such as garnet in the restite (melanosome; Vavra et al. 1996; Zeck and Whitehouse 1999). Thus, we interpret 77 Ma as the age of the peak of regional metamorphism of host gneisses.

The youngest ages are from four zircons at 47–53 Ma (fig. 6D) that are defined by analyses of crystal cores that lack zoning, that have dull CL, and that have irregular morphology. These crystals are not overgrown by any visible rim, and no 47–53-Ma rim is found on other crystals. The resorption was the final process in the morphological evolution of these crystals, significantly postdating the 77-Ma peak metamorphism. This process could have been subsolidus, either because of localized, fluid-controlled decomposition of biotite, a major reservoir of Zr (e.g., Vavra et al. 1996), or because of minor recrystallization of older zircons in veins. The regional nature of our sampling does not allow us to suggest the structural position of these youngest zircons in each hand specimen. However, since these zircons are found in both northern and southern locations, the occurrence of these isolated zircons signifies another regional thermal event at 47–53 Ma.

Ganal Massif. Thirty-one analyses were performed on 31 zircons in two samples from the GM (table 1). In a composite sample of amphibolites and one hand specimen of gabbro in the GM, zircon age distribution is much simpler than in the SM. A Tera-Wasserburg concordia diagram (fig. 7) demonstrates that most analyses are concordant within error, except for three analyses, which have a significant proportion of inherited common [207]Pb. The age histogram for amphibolites and gabbro shows two age groups, one at 60–80 Ma and one at 18–40 Ma (fig. 8).

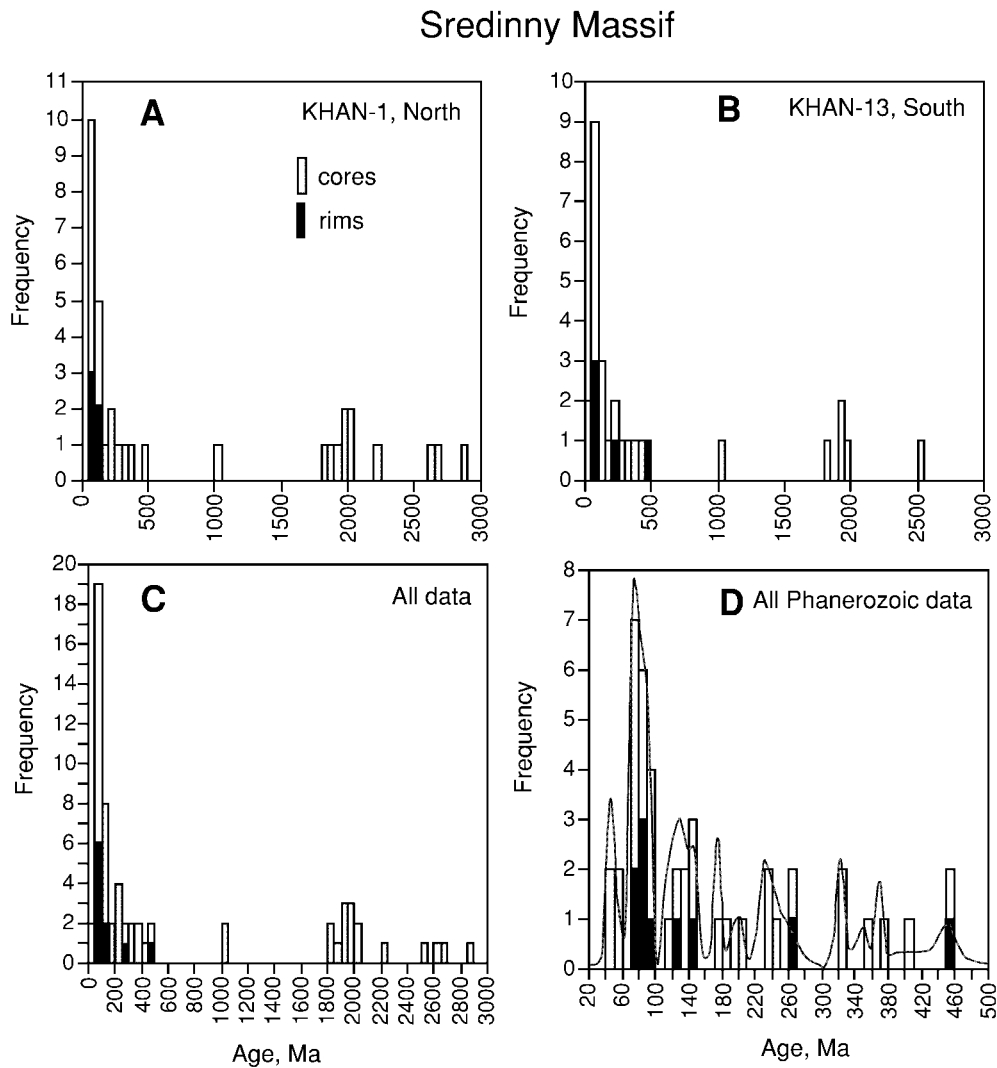Zircons in amphibolites fall into one of the fol-

Sredinny Massif

Figure 6. Histograms of age distribution in the Sredinny Massif. *A*, Sample KHAN-1 from the north of the massif. *B*, Sample KHAN-13 from the south of the massif. *C*, Cumulative age histogram. *D*, Phanerozoic part with a cumulative probability curve that accounts for errors associated with each analysis.

lowing two morphological categories: (1) smaller euhedral crystals with oscillatory zoning, without any distinct inherited cores or (2) larger anhedral crystals with planar-banded zoning, crosscutting the whole crystal, as well as complex, internally recrystallized (e.g., Vavra et al. 1996) crystals (fig. 4). No definite detrital cores are seen in any of these age groups. The zircons of the first morphological type cluster around 18–35 Ma, with no age difference between the center and edge of crystals (table 1). Anhedral zircons of the second group are exclusively 60–80 Ma. Outer parts in two anhedral crystals yield intermediate and concordant 59- and 32-Ma ages.

All zircons in gabbro-norite of the Yurchik pluton

have a euhedral, short prismatic shape and no overgrowths. Most crystals have igneous oscillatory zoning; a quarter contain dark-CL cores with irregular morphology, described as patchwork zoning, which is indicative of internal recrystallization of inherited or earlier crystallized cores (Nemchin and Pidgeon 1997). The rest do not show any preserved internal features. Tera-Wasserburg concordia ages for nine points yield 71 ± 4.3 Ma (MSWD = 15). As a result of the small size of zircons in the Yurchik pluton, it was difficult to perform quantitative analysis on the edge of single crystals. A single analysis on a light CL subhedral crystal edge gives 39 Ma, an age that is comparable to the youngest age in country rock amphibolites.
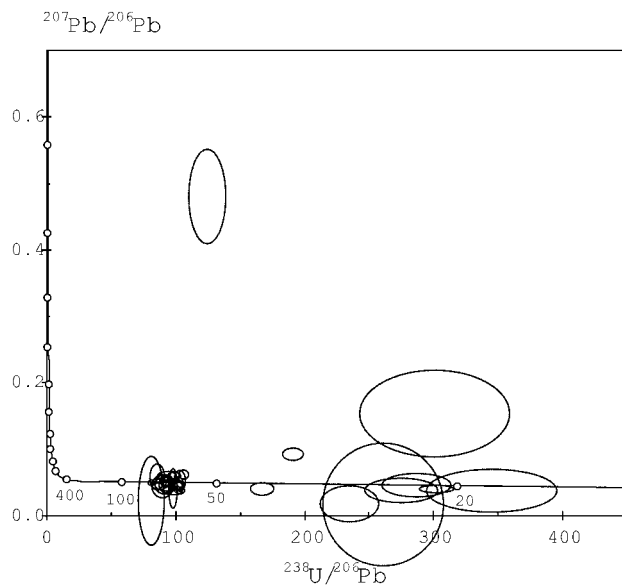
Figure 7. Tera-Wasserburg Concordia diagram for zircon analyses in amphibolites and gabbro of the Ganal Massif; $\pm 2\sigma$ ellipses are shown.

Interpretation of Zircon Age Pattern

Sredinny Massif. We interpret cores in most zircons as being detrital in origin. Qz-Pl paragneisses of the SM, whose zircon population contains more than 50% of inherited zircon cores, indicate metamorphism and, most likely, polymetamorphism (e.g., Khanchuk 1985) of a siliciclastic sedimentary protolith. The source area for the detrital cores includes a variety of rocks with ages ranging from the Archean to Cretaceous. The high percentage of zircons with Precambrian cores and the zircon age spectrum (fig. 6C) provide direct evidence for the continental nature and fingerprint the location of their source continent. In addition to zircon provenance, the following observations are critical for interpretation: (1) large thickness of siliciclastic metasedimentary units of the autochthonous complex of the SM (>2–4 km); (2) predominantly felsic terrigenous nature of all constituent series of the SM; (3) large (200 × 40 km) size of the SM, which is considered to represent the metamorphic basement of 1000 × 200-km Western Kamchatka (Bogdanov and Khain 2000) or an even larger continental block in the Sea of Okhotsk, Okhotomorsk microcontinent (Parfenov and Natal'in 1986); (4) relative similarity of lithologies and zircon age patterns in samples collected as far as 150 km apart; and (5) relatively primitive whole-rock $^{87}Sr/^{86}Sr_i$ (0.703–0.706). Together, these observations suggest that the source zircons were derived from an ex-

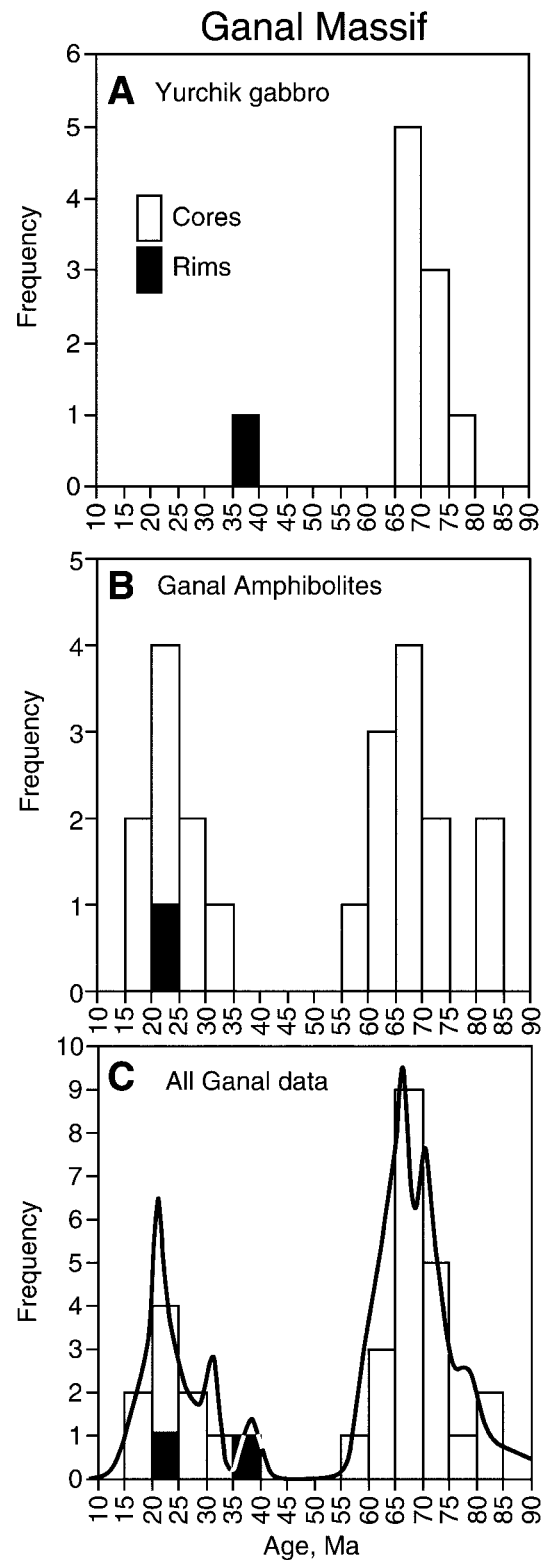**Figure 8.** Histogram of age distribution in the Ganal Massif. *A*, Gabbro norite of the Yurchik pluton. *B*, Amphibolites of the Ganal series. *C*, Cumulative age histogram with curve of cumulative probabilities.

tensive polychronous sequence of rocks from the area with a complex age pattern that was experiencing high erosion rates. Given low whole-rock $^{87}Sr/^{86}Sr_i$ values, no high-Sr Precambrian feldspars have been accumulating with the Precambrian zircons, nor does the SM represent a polymetamorphic Archean basement. Therefore, these old zircons in radiogenically immature, low-Rb/Sr rocks were deposited individually with clastic sediments in which feldspars (high-Sr, high-$^{87}Sr/^{86}Sr$ minerals) were weathered. This could suggest derivation of these oldest zircons from earlier-formed sedimentary rocks (e.g., those that form a cover on a Precambrian basement of a craton). It is possible that a series of such erosion/metamorphism/reaccumulation events has led to recycling of older zircon cores from one sedimentary/metasedimentary rock to another; this, in turn, has lead to removal of feldspars (and radiogenic Sr) and erasure of old protolith ages from the rock other than U-Pb in zircons themselves. The large abundance of Archean and Proterozoic zircon cores—19 grains, or 31% of total population—requires as a possibility the accumulation of the SM sediments in the close vicinity or on the margin of a Precambrian craton with the deeply eroded platformal cover. Another constraint is imposed by the presence of a wide variety of Paleozoic-Triassic zircons (fig. 6D) and by the youngest abundant detrital and/or volcanic cores of Late Jurassic to Early Cretaceous age. Therefore, a long-lived Phanerozoic magmatic arc on or near a Precambrian continental margin will satisfy all requirements for a source area.

If we are correct, and 120–96 Ma represents the last stage of detrital zircon deposition, then this complex age pattern suggests that paragneisses of the SM were metamorphosed after Early Cretaceous. This scenario constrains a short time (<20 m.yr.) interval between the deposition of last detrital zircon and metamorphism.

We interpret the ubiquitous episode of 77-Ma overgrowth as the main episode of high-grade regional metamorphism and migmatization that generated paragneisses of the Kolpakovskaya series; 77 Ma would fall in the middle of most whole-rock K-Ar and Rb-Sr whole-rock ages of metamorphism for the suite of samples studied here. In this interpretation, the time lag between the last sedimentary deposition of 96-Ma detrital cores and the high-grade regional metamorphism and anatexis (77-Ma rims) is only a few tens of millions of years apart, possibly less than 20 m.yr. (fig. 6D). The 47–53-Ma age of zircons corresponds to the youngest Rb-Sr internal isochron age of retrogression of the younger Malkinskaya series

metamorphic event (see appendix; Bondarenko et al. 1993; Vinogradov and Grigoryev 1994).

Ganal Massif. Ganal amphibolites largely represent metamorphosed tholeiitic basalts and greywackes (German 1978; Rikhter 1991), which do not usually contain zircons. In Ganal amphibolites, the absence of zircons older than the Late Cretaceous and the absence of any inherited cores may indicate that the mafic protolith did not contain older zircons or that no older zircon cores have survived the 66-Ma metamorphism. In the Yurchik gabbro, the initially hot and zircon-undersaturated tholeiitic magma would have likely resorbed any zircon xenocrysts, if they were entrapped from country rocks. In this respect, it is puzzling that earlier analyses of milligram-size bulk fractions indicate the presence of a discordant Archean component in zircons from amphibolites, granulites, and the Yurchik gabbro of the GM (Lvov et al. 1986). These authors propose that tens of percent of the GM zircons are Precambrian, a conclusion that is now used in many tectonic interpretations. Here, we have not found any pre-Cretaceous zircons in the GM among 31 analyzed grains. In addition, the previously proposed Archean age contradicts the rather primitive whole-rock values of $^{87}Sr/^{86}Sr =$ 0.703, more consistent with metamorphism of young oceanic crust with marine sediments (ϵ_{Nd} from −3 to +9.5; Vinogradov et al. 1991).

Therefore, we interpret the 66 ± 2-Ma zircon cores as representing the age of the high-grade metamorphism. Zircons first crystallized during this stage by using zirconium that initially resided in the altered glass and clays of parental metabasalts. The 66-Ma age is not significantly different from the crystallization age of the Yurchik gabbro (71 ± 4 Ma), consistent with the synmetamorphic origin of the gabbro (German 1978).

The 24 ± 5-Ma zircon growth/recrystallization reflects another high-grade metamorphic event that affected both the Ganal series and Yurchik gabbro. This episode can be attributed to the Stenovaya series metamorphism, which was defined earlier by German (1978) on the basis of mapping and by Mohammed et al. (1998) on the basis of metamorphic mineral assemblages (see appendix). The 24-Ma episode did not initiate zircon overgrowth on 60–80-Ma zircons but, rather, caused their significant resorption, recrystallization, and formation of new zircon crystals. Zinkevich et al. (1993) reported $^{40}Ar/^{39}Ar$ analyses on bulk samples of feldspar, amphibole, and biotite and obtained ages of 52–35 Ma, which may represent a mixture of two metamorphic events. We resolve these events here on the basis of our analyses of individual zircons.

The Origin of SM and GM and Kamchatka Accretion

The new geochronological information presented above allows us to put critical constraints on the origin of the GM and SM. The zircon provenance and the age spectra in the GM and SM are totally different, indicating that the GM and SM are not related to each other with respect to their age and protolith. These conclusions contradict the widespread opinion that the SM and GM represent the upper and lower crusts of the same terrane (e.g., Sidorenko 1964; Markov 1975; Khanchuk 1985). The SM and GM have originated and experienced metamorphism at different times and at different places.

Sredinny Massif.   The previous interpretations on the origin of the SM and Western Kamchatka are controversial. Zonenshain et al. (1990) considered both SM and GM as pieces of another continent brought to its present location from the Southern Hemisphere with the Pacific or Kula Plates. Some plateaus in the Indian Ocean do contain Precambrian crust and represent fragments of continents separated by rifting (Nicolaysen et al. 2001). Alternatively, the SM was proposed to represent an uplifted metamorphic basement of the Sea of Okhotsk, called the Okhotomorsk microcontinent (Parfenov and Natal'in 1986), for which an Asian origin is inferred (Sengör and Natal'in 1996).

Zircon provenance requires the generation of the protolith in the vicinity of a magmatic arc with the Precambrian basement, with Archean rocks, a variety of Paleozoic to Mesozoic rocks, and a short time interval (<20–40 m.yr.) between the youngest Cretaceous detrital cores (120–96 Ma) and the 77-Ma metamorphism. These constraints restrict trans-Pacific, with-the-plate transport of the SM (e.g., Zonenshain et al. 1990), given that such a short time gap would not be sufficient to rift, transport, accrete, and cause metamorphism of the SM even at a rapid 10 cm/yr plate motion. In addition, in the Late Jurassic–Early Cretaceous, the Paleo-Pacific Ocean was significantly larger (e.g., Rowley 1992). Therefore, no continent of origin will satisfy the short time available for transport other than Siberia. The position of the SM on the long-lived, active, Andean-type continental margin of Siberia would satisfy zircon provenance, polymetamorphic history, complicated folding, and thick siliciclastic sequences. Therefore, we think the SM was located on a leading edge of the Eurasian continental margin and that it provides a model for explaining how a piece of Asia that formed before the mid-Cre-

taceous could occur to the east of the Late Cretaceous subduction zone (stretching for 6000 km from Japan to North America; e.g., Parfenov and Natal'in 1986; Nokleberg et al. 1998), making SM the eastern margin of Asia.

Following Parfenov and Natal'in (1986), we infer that the SM is the eastern part of the Okhotomorsk block occupying the central part of the Sea of Okhotsk (figs. 2, 9). The chain of high-amplitude magnetic anomalies (Baboshina et al. 1984) along the northern side of the Okhotomorsk block marks the Late Cretaceous suture between the block and the Okhotsk-Chukotsk subduction margin of Asia (fig. 2). This suture was the main reason to consider the Okhotomorsk block as exotic in respect to Asia (Parfenov and Natal'in 1986; Jolivet et al. 1988; Zonenshain et al. 1990). Comparative analysis and palinspastic reconstructions of continental blocks within the Mesozoic foldbelts in the Pacific margin of Asia demonstrate that none of the blocks, including the Okhotomorsk block, are exotic in origin and that the origin of the Okhotomorsk block is explained by the scissor-like closure of the Vendian to early Mesozoic Khangai-Khantey Ocean (Sengör and Natal'in 1996). During the Paleozoic and early Mesozoic, this ocean was subducted both to the north and south (present-day coordinate) beneath the Tuva-Mongol arc (fig. 9A). The basement of the arc is made up of Riphean and older Precambrian rocks rifted off the Siberian craton (Sengör and Natal'in 1996). Voluminous subduction-accretionary complexes have been formed in front of the arc; they indicate deep and fast erosion of the arc. In the present-day structure, the Tuva-Mongol arc forms the tightly folded orocline in which the subduction-accretionary complexes are preserved in the Mongolian/Transbaikalian sector (figs. 2, 9C). The formation of the orocline started in the Permian after the collision of the Tuva-Mongol arc with the North China block. The scissor-like closure of the Khangay-Khantey ocean led to the formation of conjugated strike-slip faults and the extrusion of the forearc/arc fragments that resided in the internal part of the orocline toward the paleo-Pacific.

Sengör and Natal'in (1996) infer that these expelled fragments form the basement of the Okhotomorsk block. If the SM does belong to the Okhotomorsk block, the proposed model explains the existence of the wide spectrum of zircon ages recorded in the Kolpakovskaya series. The subduction-accretionary complexes of the Tuva-Mongol arc formed at the expense of the erosion of the Precambrian crust of the Siberian craton and the Tuva-Mongol arc as well as Paleozoic to early Mesozoic
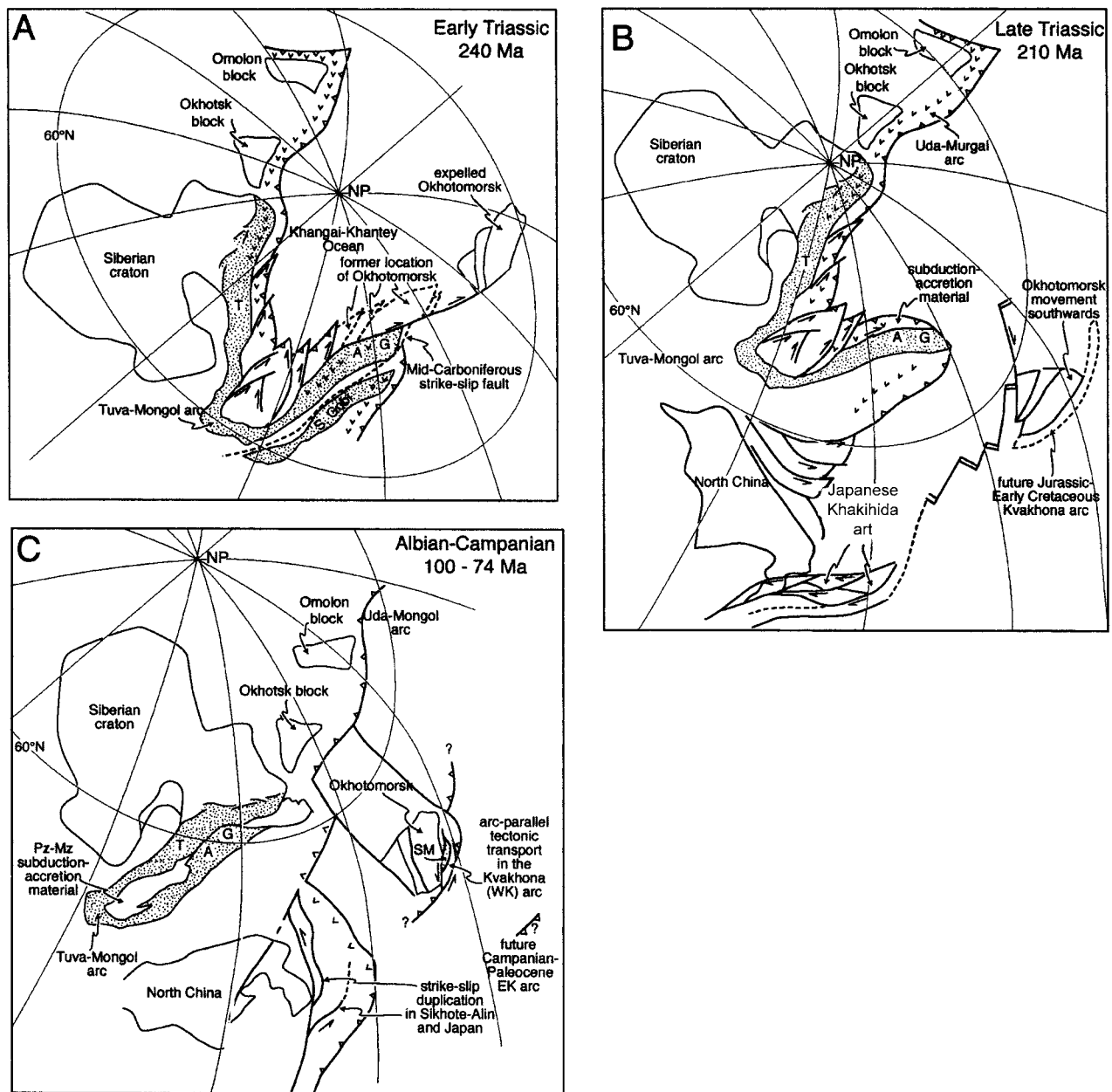
Figure 9. Origin and history of the Okhotomorsk/Sredinny Massif continental blocks (paleotectonic reconstructions modified after Sengör and Natal'in 1996). *A*, Early Triassic (240 Ma). Vendian–early Mesozoic subduction formed voluminous accretionary wedges along the Khangai-Khantey sides of the Tuva-Mongol arc. The Middle Carboniferous dextral displacement of the South Gobi segment of the Tuva-Mongol arc left behind part of its accretionary wedge, which explains the excessive volume of subduction-accretion material along the southern part of the Tuva-Mongol arc. The Late Paleozoic–Early Mesozoic scissor-like closure of the Khangai-Khantey ocean caused the extrusion of the Khangai-Khantey accretionary wedge to the east toward the paleo-Pacific. Dashed lines show the expelled part of this wedge, which forms the basement of the Okhotomorsk/Sredinny continental block. *T*, *G*, and *A* are Transbaikal, Gonzha, and Argun segments of the Tuva-Mongol arc, where the early and Late Paleozoic magmatism was widespread. *B*, Late Triassic (210 Ma). Dextral displacements established in Korea and Japan were responsible for disruption of the Khakihida arc. The same tectonic regime could move the Okhotomorsk block to the south of the "mouth" of the Khangai-Khantey ocean and thus to replace it farther away from the Triassic to Cretaceous subduction margin of northeastern Asia (Uda-Murgal arc in the figure). Note that the Kvakhona arc was formed along the southeastern margin of the Okhotomorsk block only in the Jurassic–Early Cretaceous. *C*, Albian-Campanian (100–74 Ma). The

magmatic and metamorphic rocks of the arc itself. The simplest palinspastic reconstruction requires us to place the expelled material against the Gonzha and Argun segments of the Tuva-Mongol arc (Gn and Ar in figs. 2, 9), where the early and late Paleozoic granitic magmatism was well developed. Interestingly, two peaks of zircon ages from the Kolpakovskaya series fit these magmatic events. Alternatively, zircon provenance is permissive of the SM and Okhotomorsk block originating along the north, Transbaikalian (*T* in figs. 2, 9) side of the Tuva-Mongol arc, where thousand-kilometer-long plutonic belts were developed throughout the Paleozoic and into the Early Mesozoic (e.g., Bindeman et al. 1999). However, this would require more complex kinematic history of expulsion through the closing of Khangai-Khantey ocean.

Sparse geologic data make reconstruction of the following history of the Okhotomorsk block less certain: whether it resided near the Asian margin or moved into the internal part of the paleo-Pacific remains unclear. Prolonged, Late Triassic to Cretaceous evolution of the Uda-Murgal and Okhotsk-Chukotsk arcs indicate that a considerable amount of oceanic crust has subducted beneath the Siberian margin of Asia as well as the Pacific north. This continuous subduction implies that the position of the Okhotomorsk block now juxtaposing this subduction zone was to the south to permit subduction of oceanic crust. Triassic right-lateral, orogen-parallel, strike-slip faults have been documented in Korea and Japan (see Sengör and Natal'in 1996 and references therein). They were responsible for disruption of the Late Paleozoic to Early Triassic Khakihida arc (fig. 9*B*) and dispersion of its fragments along the eastern margin of Asia. Obviously this event had to be controlled by regional plate kinematics. We infer that the Okhotomorsk block could be placed farther to the south after being expelled from the Khangai-Khantey ocean (fig. 9*B*).

Structural relationships in Western Kamchatka (Bondarenko and Sokolov 1990; Remizovsky et al. 1993; Konstantinovskaya 2000), magnetic and gravity data, and dragging on the southeastern parts of the Okhotomorsk block (Sergeev and Krasny 1987)

allow the inference that the Late Jurassic–Early Cretaceous Kvakhona arc was constructed atop and along the eastern side of the Okhotomorsk block (fig. 9*B*).

From the regional framework, the subduction beneath the Okhotomorsk/SM continental block is the simplest solution for estimation of the polarity of the Kvakhona arc. Sedimentation in the forearc region of this arc was controlled by erosion of both the arc and the underlying basement. The Tuva-Mongol population of zircons (older than Jurassic) from the basement could be redeposited and mixed with the newer (180–96 Ma) volcanic zircons that arrived from the Kvakhona arc. All researchers agree on complex structure and polymetamorphism of the Kolpakovskaya series. It is not clear whether this series represents new additions to the Okhotomorsk/SM block that formed as a result of the Kvakhona arc activity or if it is a tectonic mixture of this new material and the older basement. Redeposition of zircons is possible because the Malkinskaya series overlying the Kolpakovskaya series and containing clasts of metamorphic and magmatic rocks from the Kolpakovskaya series yields an age spectrum of detrital zircons (Hourigan et al. 2001) that is similar to the zircon ages of the Kolpakovskaya series.

Thrust-bounded slices of the Kvakhona arc form a left-stepping en echelon array in Aptian-Maastrichtian turbidites (Bondarenko and Sokolov 1990; Remizovsky et al. 1993), which implies that left-lateral, strike-slip motion was active during or immediately after the formation of the Kvakhona arc. This tectonic regime could separate the SM together with the Kvakhona arc from the main body of the Okhotomorsk block and replace it to the north (fig. 9*C*). Large-scale, left-lateral, strike-slip duplication of the Jurassic to early Cretaceous accretionary complexes synchronous to subduction has been established in the Sikhote-Alin/Japan sector of the Pacific margin of Asia (Natal'in 1993). In the Koryak region of northern Kamchatka, the en echelon pattern of tectonic units also suggests that the same left-lateral regime of displacement characterized the entire Pacific margin of northern Asia

mid-Cretaceous is the time of strike-slip duplication of the Sikhote-Alin and Japan middle Jurassic to earliest Cretaceous accretionary complexes resulting from the oblique subduction of the Paleo-Pacific plates beneath the Asian margin, and we suggest that the Kvakhona arc had the same kinematic history. The transition from subduction to strike-slip motion stopped growth of the accretionary prism and underplating of the subduction-accretion material. Detrital zircons younger then 96 Ma could not get into zone of metamorphism where Kolpakovskaya series was formed. The strike-slip faulting partly separated SM from the Okhotomorsk block. The exhumation of the high-grade Kolpakovskaya series rocks at 77 Ma is related to the extension resulting from arc-parallel tectonic transport.

during the Late Cretaceous (Sengör and Natal'in 1996).

The long-lasting, arc-parallel tectonic transport along the Pacific side of northern Asia is important for understanding the tectonic history of Kamchatka for two reasons. First, this tectonic regime may explain the time gap between the youngest detrital zircon ages (96 Ma) and regional metamorphism of the Kolpakovskaya series at 77 Ma. Low $^{87}Sr/^{86}Sr_i$ values of rocks allow inference that the main bulk of the Kolpakovskaya series is subduction-accretion material added to the Kvakhona arc. Subduction is the most reliable mechanism for placing this material to the depths of kyanite-grade metamorphism. Second, regional metamorphism of the Kolpakovskaya series at 77 Ma happened earlier than the late Paleocene–early Eocene collision of the Eastern Kamchatka intraoceanic arc (Konstantinovskaya 2001). Thus, we infer that exhumation of the high-grade metamorphic rocks of the Kolpakovskaya series was related to the strike-slip tectonics caused by oblique subduction. Tectonic setting within extending arcs (McCaffrey 1996) or changes of the obliquity of convergence along the arc (Ave Lallement and Guth 1990) can cause the exhumation of deep-seated rocks.

We view the less intensive 47–53-Ma episode of zircon growth as evidence for another superimposed metamorphism: the metamorphism resulted from renewed subduction and burial, and the burial itself resulted from collision with Eastern Kamchatka. In this scenario, subduction under the Western Kamchatka has never stopped, but the position of the SM relative to the volcanic front (and magma supply) was not always favorable to sustain conditions for metamorphism and for the new zircon growth and recycling.

Ganal Massif.   Our view on the origin of the GM is largely consistent with the proposed tectonic models and their sequence of events (e.g., Geist et al. 1994; Garver et al. 2000; Konstantinovskaya 2000). The absence of older zircons in GM, the tholeiitic character of its protolith volcanics, intraoceanic character of its sediments, and zircon age spectrum all support the interpretation that the protolith for the GM was generated as an ocean arc, away from a large continental mass. Furthermore, the paleomagnetic data are consistent with the hypothesis that GM originated in the south of its present location (e.g., Konstantinovskaya 2000) and was carried by the Pacific or Kula plate. The 71-Ma intrusion of the Yurchik gabbro and the 66-Ma zircon growth in Ganal metagraywackes would, then, correspond to an intraoceanic arc magmatism/metamorphism and deformation and could be consistent

with inferred intraoceanic plate reorganization (e.g., Konstantinovskaya 2000). The youngest 24-Ma age of zircon growth event in the GM is entirely postaccretional. This episode is closely linked in time and space with the Miocene accretion of Eastern Peninsulas terranes that are tectonically overthrust on Eastern Kamchatka (see fig. 2; Geist et al. 1994; Soloviev et al. 1998; Levashova et al. 2000).

Conclusions

1. The Sredinny and Ganal Massifs, despite their present adjacent position, represent two different tectonic units and were never upper and lower crustal levels of the same unit.

2. The Sredinny Massif, as the metamorphic basement of the Western Kamchatka, contains detrital zircons with a wide age spectrum from 2800 to 96 Ma. The Archean, Proterozoic, and Paleozoic zircons came from source areas in Siberia. This discovery contradicts the widely accepted opinion about exotic, extra-Asian origin of the Sredinny Massif and the Okhotomorsk block to which this massif belongs. Two episodes of metamorphism and zircon growth are identified: 77 and 47–53 Ma. The 77-Ma regional metamorphism and migmatization in SM is interpreted to reflect an intra-arc transtensional deformation, and 47–53-Ma metamorphism is syncollisional and related to the accretion of Eastern Kamchatka.

3. The Ganal Massif, as the metamorphic basement of the Eastern Kamchatka, could have originated in an intraoceanic island arc setting and been transported to its present position by the Pacific or Kula plate. No old, continent-derived zircons were found, and two episodes of zircon growth at 66 and 24 Ma are interpreted to represent regional metamorphisms. The first metamorphism is related to intraoceanic arc growth and/or reorganization, and the second reflects a superimposed metamorphism after accretion resulting from renewed subduction.

4. To explain the appearance of the old Siberian zircons in the Sredinny Massif located to the east of the well-defined and extended subduction zone that marked the eastern margin of Siberia in the Cretaceous, we propose a model that includes: (*a*) formation of the Okhotomorsk-Sredinny Massif continental block as a result of the eastward extrusion of the subduction-accretion material that happened during the Triassic closure of the Khangai-Khantey ocean, (*b*) formation of the Jurassic–Early Cretaceous Kvakhona arc along the eastern side of this continental block and redeposition of the older zircons in its forearc region, (*c*) northward displacement of the block toward the Okhotsk-Chukotka

subduction zone, and (*d*) arc-parallel tectonic transport within the Kvakhona arc that was responsible for exhumation of the high-grade rocks.

R E F E R E N C E S   C I T E D

Ave Lallemant, H. G., and Guth, L. R. 1990. Role of extensional tectonics in exhumation of eclogites and blueschists in an oblique subduction setting: northeastern Venezuela. Geology 18:950–953.

Baboshina, V. A.; Tereschenkov, A. A.; and Kharakhinov, V. V. 1984. Deep structure of the Sea of Okhotsk according to geophysical data, overview information. Vsesouzniy Nauchno-Issledovatelskiy Institute (VNII) Gazprom 3:41 (in Russian).

Baranov, B. V.; Seliverstov, N. I.; Muratov, A. V.; and Muzuzov, E. L. 1991. The Komandorsk basin as a product of spreading behind a transform plate boundary. Tectonophysics 199:237–269.

Beck, M. E., Jr. 1986. Coastwise transport reconsidered: lateral displacements in oblique subduction zones, and tectonic consequences. Phys. Earth Planet. Int. 68:1–8.

———. 1991. Model for late Mesozoic–early Tertiary tectonics of coastal California and western Mexico and speculation on the origin of the San Andreas Fault. Tectonics 5:49–64.

Bindeman, I. N.; Davis, A. M.; and Wickham, S. M. 1999. 400 Ma of magmatism evolution in a single lithospheric bloc during cratonization: ion microprobe study of relict plagioclase megacrysts in mafic rocks from Transbaikalia, Russia. J. Petrol. 40:807–830.

Bogdanov, N. A., and Khain, V. E., eds. 2000. Tectonic map of the sea of Okhotsk region: map and explanatory notes, scale 1 : 2,500,000. Moscow, Nedra.

Bondarenko, G. E.; Kuznetsov, N. B.; Savostin, L. A.; Smolyar, M. I.; and Sokolov, S. Y. 1993. Isotope age of garnet plagiogranitoids of Middle Kamchatka. Trans. Russ. Acad. Sci. Earth Sci. Sect. 330:233–236.

Bondarenko, G. E., and Sokolkov, V. A. 1990. New data on the age, structure and depositional environment of volcanic-siliceous-carbonate complex of the Omgon cape (western Kamchatka). Trans. Russ. Acad. Sci. Earth Sci. Sect. 315/316:1434–1437.

Engebretson, D. C.; Cox, A.; and Gordon, R. G. 1985. Relative motions between oceanic and continental plates in the Pacific basin. Geol. Soc. Am. Spec. Pap. 206, 59 p.

Faure, M.; Lalevee, F.; Gusokujima, Y.; Iiyama, J.-T.; and Cadet, J.-P. 1986. The pre-Cretaceous deep-seated tectonics of the Abukuma massif and its place in the structural framework of Japan. Earth Planet. Sci. Lett. 77:386–398.

Gaedicke, C.; Baranov, B.; Seliverstov, N.; Alexeiev, D.; Tsukanov, N.; and Freitag, R. 2000. Structure of an active arc-continent collision area: the Aleutian-Kamchatka junction. Tectonophysics 325:63–85.

Garver, J. I.; Soloviev, A. V.; Bullen, M. E.; and Brandon, M. T. 2000. Towards a more complete record of magmatism and exhumation in continental arcs, using detrital fission-track thermochronology. Phys. Chem. Earth 25A:565–570.

Geist, E. L.; Vallier, T. L.; and Scholl, D. W. 1994. Origin, transport and emplacement of an exotic island arc terrane exposed in eastern Kamchatka, Russia. Geol. Soc. Am. Bull. 106:1182–1194.

German, L. L. 1978. Ancient crystalline complexes of Kamchatka. Moscow, Nedra, 128 p. (in Russian).

Gnibudenko, G. S., and Khvedchuk, I. I. 1982. Main tectonic features of the Sea of Okhotsk. *In* Geologicheskoe stroenie Okhotomorsk regiona [Geological structure of the Okhotomorsk region]. Vladivostok, Far East Scientific Center, p. 3–25 (in Russian).

Hourigan, J. K.; Brandon, M. T.; Garver, J. I.; and Soloviev, A. V. 2001. A comparison of the detrital zircon grain-age distributions from Ukelayat group and the Kamchatskiy complex of the Sredinny Range, Kamchatka. 7th Zonenshain International Conference on Plate Tectonics (2001, Moscow-St. Petersburg, Russia). Nauchuny Mir. Workshop 2. *In* N. A. Bogdanov, ed. Tectonics and the Sea of Okhotsk Region and Kamchatka. Abstracts and Programs, 504 p.

Jolivet, L.; Cadet, J. P.; and Lalevee, F. 1988. Mesozoic evolution of northeast Asia and the collision of the Okhotsk microcontinent. Tectonophysics 149:89–109.

Jolivet, L.; Tamaki, K.; and Fournier, M. 1994. Japan Sea, opening history and mechanism—a synthesis. J. Geophys. Res. 99:22,237–22,259.

Khanchuk, A. 1985. Evolution of ancient sialic crust in island-arc system of eastern Asia. Vladivostok, Academy of Sciences of the USSR, Far East Scientific Center, Far East Geological Institute. 137 p. (in Russian).

Kimura, G. 1994. The latest Cretaceous–early Paleogene rapid growth of accretionary complex and exhumation of high pressure series metamorphic rocks in NW Pacific margin. J. Geophys. Res. 99:22,147–22,164.

Konstantinovskaya, E. A. 2000. Geodynamics of an Early Eocene arc-continent collision reconstructed from Kamchatka Orogenic Belt, NE Russia. Tectonophysics 325:87–105.

———. 2001. Arc-continent collision and subduction reversal in the Cenozoic evolution of the northwest Pacific: an example from Kamchatka (NE Russia). Tectonophysics 333:75–94.

Levashova, N. M.; Shapiro, M. N.; Beniamovsky, V. N.; and Bazhenov, M. L. 2000. Paleomagnetism and geochronology of the Late Cretaceous–Paleogene island arc complex of the Kronotsky Peninsula, Kamchatka, Russia: kinematic implications. Tectonics 19:834–851.

Ludwig, K. R. 2000. ISOPLOT. Version 2.3. Berkeley Geochronology Center, special publication 1a.

Lvov, A. B.; Neelov, A. N.; Bogomolov, E. S.; and Mikhailova, N. S. 1986. On the age of the metamorphic rocks of the Ganalsky Range, Kamchatka. Sov. Geol. Geophys. N7:47–56.

Markov, M. C. 1975. Metamorphic complexes and "basaltic layer" of the crust of island arcs. Moscow, Nauka, 232 p. (in Russian).

McCaffrey, R. 1996. Estimates of modern arc-parallel strain rates in fore arcs. Geology 24:27–30.

Mohammed, H.-A.; Feldman, V. I.; and Kastrikina, V. M. 1998. Condition of formation for metamorphic rocks of Ganal blok (Kamchatka). Vestnik Moscow State University, ser. 4, Geology N2:23–30 (in Russian).

Natal'in, B. A. 1993. History and mode of Mesozoic accretion in southeastern Russia. Island Arc 2:15–34.

Natal'in, B. A.; Parfenov, L. M.; Vrublevsky, A. A.; Karsakov, L. P.; and Yushmanov, V. V. 1986. Main fault systems of the Soviet Far East. Philos. Trans. R. Soc. Lond. A Math. Phys. Sci. 317:267–275.

Nemchin, A., and Pidgeon, R. T. 1997. Evolution of the Darling Range batholith, Yilgarn Craton, western Australia: a SHRIMP zircon study. J. Petrol. 38:625–649.

Nicolaysen, K.; Bowring, S.; Frey, F.; Weis, D.; Ingle, S.; Pringle, M. S.; and Coffin, M. F. 2001. Provenence of Proterozoic garnet-biotite gneiss recovered from Elan Bank, Kerguelen Plateau, south Indian Ocean. Geology 29:235–238.

Nokleberg, W. J.; Parfenov, L. M.; Monger-James, W. H.; Norton, I. O.; Khanchuk, A. I.; Stone, D. B.; Scholl, D. W.; and Fujita, K. 1998. Phanerozoic tectonic evolution of the circum-north Pacific. U.S. Geologic Survey (USGS) open-file report 98-754. Menlo Park, Calif., USGS, 125 p.

Paces, J. B., and Miller, J. D. 1993. U-Pb ages of Duluth complex and related mafic intrusions, north-eastern Minnesota: geochronologic insights to physical, petrogenetic, paleomagnetic, and tectonomagmatic processes associated with the 1.1 Ga mid-continent rift system. J. Geophys. Res. 98:13,997–14,013.

Parfenov, L. M., and Natal'in, B. A. 1986. Mesozoic tectonic evolution of NE Asia. Tectonophysics 127:291–304.

Parfenov, L. M.; Voinova, I. P.; Natal'in, B. A.; and Semenof, D. F. 1978. Geodynamics of north-eastern Asia in Mesozoic and Cenozoic time and the nature of volcanic belts. J. Phys. Earth 26(suppl.):S503–S525.

Remizovsky, R. I.; Bondarenko, G. E.; Sokolkov, V. A.; and Sidorov, V. A. 1993. New data on paleomagnetism

of Middle Jurassic to Cretaceous complexes in western Kamchatka. Vestnik of the Moscow State University, ser. 4, Geology 3:82–87 (in Russian).

Rikhter, A. V. 1991. Structure of metamorphic complexes in the Ganal Range, Kamchatka Massif. Geotectonics N1:98–108.

———. 1995. Structure of metamorphic complexes of the Sredinny Kamchatka Massif. Geotectonics N1:71–78.

Rowley, D. B. 1992. Reconstruction of the Circum Pacific region. In Westernman, G. E. G., ed. The Jurassic of the Circum Pacific. Cambridge, Cambridge University Press, p. 15–27.

Sant Blanquat, M.; Tikoff, B.; Teyssier, C.; and Vigneresse, J.-L. 1998. Transpressional kinematics and magmatic arcs. In Holdsworth, R. E.; Strachan R. A.; and Dewey, J. F., eds. Continental transpressional and transtensional tectonics. Geol. Soc. Lond. Spec. Publ. 135:327–340.

Schaltegger, U.; Fanning, C. M.; Gunther, D.; Maurin, J. C.; Schulmann, K.; and Gebauer, D. 1999. Growth, annealing and recrystallization of zircon and preservation of monazite in high-grade metamorphism: conventional and in-situ U-Pb isotope, cathodoluminescence and microchemical evidence. Contrib. Mineral. Petrol. 134:186–201.

Sengör, A. M. C., and Natal'in, B. A. 1996. Paleotectonics of Asia: fragments of a synthesis. In Yin, A., and Harrison, T. M., eds. Tectonics evolution of Asia. Cambridge, Cambridge University Press, p. 486–640.

Sergeev, K. F., and Krasny, M. L. 1987. Geology-geophysical atlas of the Kuril-Kamchatka island arc system. Leningrad, Vsesoyuznyy Nauchno-Issledovatelskiy Geologicheskiy Institut (VSEGEI), 36 sheets.

Sidorenko, A. V., ed. 1964. Kamchatka, Kurile, and Komandor Islands: geological description. In Geology of the USSR. Vol. 31. Moscow, Nedra, 733 p.

Soloviev, A. V.; Brandon, M. T.; Garver, J. I.; and Bogdanov, N. A. 1998. Collision of the Olyutorsky island arc with Eurasian continental margin: kinematics and timing. Trans. Russ. Acad. Sci. Earth Sci. Sect. 360:666–668.

Taira, A.; Tokuyama, H.; and Soh, W. 1989. Accretion tectonics and evolution of Japan. In Ben-Avraham, Z., ed. Evolution of the Pacific Ocean margins. Oxford, Oxford University Press, p. 100–123.

Vavra, G.; Gebauer, D.; Schmid, R.; and Compston, W. 1996. Multiple zircon growth and recrystallization during polyphase Late Carboniferous to Triassic metamorphism in granulites of the Ivrea zone (southern Alps): an ion microprobe (SHRIMP) study. Contrib. Mineral. Petrol. 122:337–358.

Vinogradov, V. I.; Buyakaite, M. I.; Goroshenko, G. L.; Lukanin, A. O.; and Pokrovsky, B. G. 1991. Isotope and geochronological features of deeply metamorphosed rocks of Ganal Massif in Kamchatka. Trans. Russ. Acad. Sci. Earth Sci. Sect. 318:929–936.

Vinogradov, V. I., and Grigoryev, V. S. 1994. Rb-Sr ages of Middle metamorphic block in Kamchatka. Trans. Russ. Acad. Sci. Earth Sci. Sect. 339:645–649 (English edition: 343A:80–86).

Vinogradov, V. I.; Grigoryev, V. S.; and Leytes, A. M. 1988. Age of metamorphism of the Sredinnyl Ridge of Kamchatka. Izv. Akad. Nauk. SSSR Ser. Geol. 9:30–38 (in Russian).

Volynets, O. N.; Ermakov, V. A.; and Koloskov, A. V. 1987. Inclusions in volcanic rocks of Kurile-Kamchatka island arc and their importance for understanding of petrogenesis. *In* Petrology and geochemistry of island arcs and marginal seas. Moscow, Nauka, p. 293–312 (in Russian).

Vsesouzniy Geologicheskiy Institute (VSEGEI). 1981. Geological map of Kamchatka, scale 1 : 1,000,000. Leningrad, VSEGEI.

Watson, B. F., and Fujita, K. 1985. Tectonic evolution of Kamchatka and the Sea of Okhotsk and implications for the Pacific Basin. *In* Howell, D. G., ed. Tectono-stratigraphic terranes of the Circum-Pacific region. Houston, Circum-Pacific Council for Energy and Mineral Resources, p. 333–348.

Zeck, H. P., and Whitehouse, M. J. 1999. Hercynian, Pan-African, Proterozoic and Archean ion-microprobe zircon ages for Beltic-Rif core complex, Alpine belt, W. Mediterranean—consequences for its P-T-t path. Contrib. Mineral. Petrol. 134:134–149.

Zinkevich, V. P.; Rikhter, A. B.; and Fuzgan, M. M. 1993. A ^{40}Ar/^{39}Ar dating of metamorphic rocks of eastern Kamchatka. Trans. Russ. Acad. Sci. Earth Sci. Sect. 333:477–480.

Zonenshain, L. P.; Kuzmin, M. I.; and Natapov, L. M. 1990. Geology of the USSR: a plate tectonic synthesis (English ed.). Geodynamics series 21. Washington, D.C., AGU, 242 p.